



Research article

Elevated ADAR expression is significantly linked to shorter overall survival and immune infiltration in patients with lung adenocarcinoma

Siqi Hu[†], Fang Wang[†], Junjun Yang and Xingxiang Xu*

Northern Jiangsu People's Hospital, Clinical Medical College of Yangzhou University, Yangzhou 225001, China

* **Correspondence:** Email: xuxx63@sina.com; Tel: +8618051062315.

† These two authors contributed equally.

Abstract: To date, few studies have investigated whether the RNA-editing enzymes adenosine deaminases acting on RNA (ADARs) influence RNA functioning in lung adenocarcinoma (LUAD). To investigate the role of ADAR in lung cancer, we leveraged the advantages of The Cancer Genome Atlas (TCGA) database, from which we obtained transcriptome data and clinical information from 539 patients with LUAD. First, we compared ADAR expression levels in LUAD tissues with those in normal lung tissues using paired and unpaired analyses. Next, we evaluated the influence of ADARs on multiple prognostic indicators, including overall survival at 1, 3 and 5 years, as well as disease-specific survival and progression-free interval, in patients with LUAD. We also used Kaplan-Meier survival curves to estimate overall survival and Cox regression analysis to assess covariates associated with prognosis. A nomogram was constructed to validate the impact of the ADARs and clinicopathological factors on patient survival probabilities. The volcano plot and heat map revealed the differentially expressed genes associated with ADARs in LUAD. Finally, we examined ADAR expression versus immune cell infiltration in LUAD using Spearman's analysis. Using the Gene Expression Profiling Interactive Analysis (GEPIA2) database, we identified the top 100 genes most significantly correlated with ADAR expression, constructed a protein-protein interaction network and performed a Gene Ontology/Kyoto Encyclopedia of Genes and Genomes analysis on these genes. Our results demonstrate that ADARs are overexpressed in LUAD and correlated with poor patient prognosis. ADARs markedly increase the infiltration of T central memory, T helper 2 and T helper cells, while reducing the infiltration of immature dendritic, dendritic and mast cells. Most immune

response markers, including T cells, tumor-associated macrophages, T cell exhaustion, mast cells, macrophages, monocytes and dendritic cells, are closely correlated with ADAR expression in LUAD.

Keywords: ADAR; lung adenocarcinoma (LUAD); prognostic biomarker; overall survival; immune infiltration

Abbreviations: LUAD: Lung adenocarcinoma; OS: Overall survival; ADAR: Adenosine deaminase acting on RNA; RNA-seq: RNA-sequencing; ADARB1: Adenosine Deaminase RNA Specific B1; IFN: Interferon; TCGA: The Cancer Genome Atlas; TPM: Transcripts per million; ROC: Receiver operating characteristic; DSS: Disease-specific survival; PFI: Progression-free interval; DEG: Differentially expressed gene; PPI: Protein-protein interaction; GO: Gene ontology; KEGG: Kyoto Encyclopedia of Genes and Genomes; AUC: Area under the curve; lncRNA: Long non-coding RNA; dsRNA: Double-stranded RNA; ICBs: Immune checkpoint blockers

1. Introduction

Lung cancer is at the forefront of fatal malignancies worldwide, with LUAD accounting for the most prevalent pathological type [1]. Despite significant progress in personalized treatment modalities such as targeted therapy and immunotherapy, advanced lung cancer often presents a daunting prognosis, with a 5-year OS rate of only 16% [2]. In recent years, several emerging non-invasive technologies, such as optical coherence tomography and scanning laser imaging, have been utilized for the detection of early-stage lesions. These technologies show great potential in treating diseases involving the retina, intraluminal tumors, skin tumors, among others. However, further investigation is required in the context of lung cancer [3,4]. Suboptimal screening techniques and limited reliable biomarkers typically result in late-stage diagnosis, consequently increasing mortality rates [5]. Even patients that undergo radical resection for stage I disease face a 30% risk of relapse, highlighting the continued risk of recurrence in non-small cell lung cancer post-surgery. Therefore, accurate prediction of patient outcomes is of utmost importance to enable informed decisions regarding adjuvant treatment measures [6,7]. Discovery of novel biomarkers enables identifying and tracking molecules related to tumor development and progression, and is a cornerstone of early detection, prognostic assessment and effective management of patients with lung cancer.

RNA editing is a ubiquitous biological process that occurs across mammals, enabling the introduction of base changes, such as ADAR-mediated A-to-I editing, into transcripts. Through this process, specific sites in the coding and non-coding regions of RNA sequences are modified, resulting in the production of enriched proteomes and transcriptomes [8]. Owing to the numerous RNA-seq datasets generated by high-throughput sequencing platforms, it has become possible to explore this editing at an unprecedented level of detail. Studies have discovered hundreds of millions of editing sites in human DNA, revealing the importance of RNA editing in the maintenance of biological homeostasis [9]. So far, two catalytically active enzymes involved in this process have been identified in mammals, namely ADARs (ADAR1s) and ADARB1s (ADAR2s) [10]. Several past studies have underscored the paramount importance of ADAR1-mediated RNA editing events occurring in non-coding regions as key regulators of innate immune system homeostasis and defense responses. Moreover, the ADAR-induced editing of specific double-stranded RNA blocks MDA5 recognition by

foreign elements, thereby preventing potentially harmful internal immune responses [11–13]. Interestingly, both enzymes operate and tune edited RNA molecules in a very complex and cell-specific manner, affecting the splicing, localization, translation and stability of edited RNAs within cells, potentially influencing transcriptional outputs at the molecular and organismal levels.

ADARs are widely expressed in the nervous system, demonstrating their importance in maintaining normal nervous system functions. Mutations in ADAR have been linked to rare neurological conditions, including Aicardi-Goutières syndrome and hereditary symmetry dyschromatosis [14–16]. In recent years, mounting scientific evidence from both *in vitro* and *in vivo* studies has shed light on the multifaceted roles of ADARs in tumor proliferation, invasion, metastasis and other cancer-related behaviors [17–19]. Remarkably, ADAR1 knockout appeared to sensitize tumor cells to IFN- γ and increase immune infiltration in tumor tissues, thus contributing to enhanced immunotherapy efficacy and overcoming tumor immune checkpoint inhibitor resistance [20–22]. Although the notion that elevated ADAR levels contribute to the progression of various cancers has gained acceptance, the precise involvement of ADAR in the dynamics of lung cancer is yet to be thoroughly examined. Here, we conducted a study to investigate the immunological and prognostic implications of ADAR expression in LUAD using data from TCGA. Our study provides novel insights into the molecular mechanisms underlying the involvement of ADAR in LUAD progression and highlights its potential as a therapeutic target for improving clinical outcomes.

2. Materials and methods

2.1. Patient data sets

Clinical information and RNA-seq data, expressed as TPM values, were procured from TCGA database, a publicly accessible platform for multi-cancer data. We included data from 539 patients diagnosed with LUAD, including 59 patients with matched adjacent normal tissues. The UCSC Xena platform was used to extract bulk RNA-seq data, normalized to TPM units, of LUAD tissues from TCGA and normal lung tissues from genotype-tissue expression (GTEx) datasets [23]. The cohort of patients was divided into two groups, namely high- and low-ADAR expression groups, using the median expression value of ADAR as a threshold, while utilizing publicly available datasets in a manner that complies with specified guidelines. We do not require ethical committee approval.

2.2. ADAR expression in LUAD

Initially, we employed the Mann-Whitney U test to examine ADAR expression patterns across multiple cancer types. Subsequently, we performed simultaneous paired and unpaired analyses to elucidate the possible dysregulated expression of ADAR in both LUAD and healthy lung tissues. Visual representations of the results were presented using box and line plots. Using the Human Protein Atlas (HPA) database, which provides a detailed account of protein distribution in human organs and cells [24], we examined variations in ADAR protein expression in lung cancer. In addition, we utilized the robust statistical tools provided by the R packages “pROC” and “ggplot2” to perform ROC curve analysis.

2.3. Role of ADAR in LUAD patient survival

Kaplan-Meier survival analysis was performed to investigate the relationship between ADAR expression levels and the survival rate of patients with LUAD. To delineate the optimal cutoff points, we utilized the “surv-cutoff” function available in the “Survminer” R package. Using the “timeROC” package, we analyzed the clinical prognostic data of LUAD to assess the predictive capability of the ADAR expression for OS, DSS and PFI at 1-, 3- and 5-year intervals. The findings were visualized using “ggplot2” package in R software version 4.2.1. Subsequently, we conducted Cox regression analysis to explore the potential risk factors that may influence the survival outcomes of patients with LUAD. Univariate analysis was initially performed to identify prognostic factors with a significance level of less than 0.1, followed by multivariate analysis to confirm the independent prognostic determinants. Survival curves were generated using the R package “survminer,” while nomograms and calibration curves were constructed using the “Rms” R package and the “Survival” R package. To assess the discriminatory capability of the nomogram, we calculated the concordance index (C-index) using the bootstrap resampling method with 1000 replications.

2.4. DEGs based on ADAR expression levels

Differential analysis was performed on the high- and low-ADAR expression groups using the DESeq2 package, with a threshold value of $|\log_{2}FC| > 1.5$ and adjusted $p < 0.05$ to select for DEGs. Volcano plots and heat maps were used to visualize differential gene expression patterns. This process was conducted using R software, specifically utilizing the “ggplot” and “ComplexHeatmap” functions to accomplish the respective tasks.

2.5. Immune infiltration analysis

First, the infiltration of 24 immune cell types in LUAD were identified by single-sample gene set enrichment analysis (ssGSEA) using the R package GSVA [25]. Subsequently, relevance analysis between immune cell infiltration and ADAR expression was performed using Spearman’s analysis. The results were visually depicted using the “ggplot2” package to create lollipop charts and scatter plots showing the correlation between variables and the immune infiltration matrix data.

2.6. PPI network and GO/KEGG analyses

The GEPIA2 database enabled us to explore gene interaction pathways by analyzing a vast number of tissue specimens [26]. Therefore, we extracted the top 100 genes that were closely related to ADAR and inputted the list into the STRING website to generate a PPI network diagram. The visualization of the interaction network among these 100 genes was conducted using the Cytoscape software. Furthermore, identification of hub genes, determination of clustering and evaluation of corresponding scores were performed using the Mcode plugin. Furthermore, extensive GO and KEGG analyses were conducted for these genes using the clusterProfiler package.

3. Results

3.1. Clinical characteristics

Using TCGA, we procured clinical information and transcriptome sequencing data from 539 patients with lung cancer prior to April 2023. As shown in Table 1, the patient population was divided into two groups based on ADAR expression levels, with 269 and 270 individuals in the high- and low-expression groups, respectively. The clinical characteristics examined included age, sex, race, number of years smoked, TNM stage, pathological stage, location within the lung, residual tumor, primary therapy outcome, DSS events and PFI events. Apart from race, minimal differences were observed between the clinical characteristics of the patients with high- and low-ADAR expression. Notably, there were no discernible differences in the expression of ADAR between the sexes.

Table 1. Baseline demographic and clinical features of patients with LUAD.

Characteristics	Low expression of ADAR	High expression of ADAR	P value
n	269	270	
Age, n (%)			0.998
<= 65	127 (24.4%)	130 (25%)	
> 65	130 (25%)	133 (25.6%)	
Sex, n (%)			0.092
Female	154 (28.6%)	135 (25%)	
Male	115 (21.3%)	135 (25%)	
Race, n (%)			0.006
Asian	2 (0.4%)	6 (1.3%)	
White	198 (41.9%)	211 (44.7%)	
Black or African American	38 (8.1%)	17 (3.6%)	
Number of years smoked, n (%)			0.557
< 40	93 (25.2%)	95 (25.7%)	
>= 40	84 (22.8%)	97 (26.3%)	
Pathologic T stage, n (%)			0.075
T1	98 (18.3%)	78 (14.6%)	
T2&T3&T4	171 (31.9%)	189 (35.3%)	
Pathologic N stage, n (%)			0.083
N0	186 (35.6%)	164 (31.4%)	
N1&N2&N3	78 (14.9%)	95 (18.2%)	
Pathologic M stage, n (%)			0.099
M0	179 (45.9%)	186 (47.7%)	
M1	8 (2.1%)	17 (4.4%)	
Pathologic stage, n (%)			0.165
Stage I& Stage II	215 (40.5%)	206 (38.8%)	
Stage III& Stage IV	48 (9%)	62 (11.7%)	
Primary therapy outcome, n (%)			0.116

Continued on next page

Characteristics	Low expression of ADAR	High expression of ADAR	P value
PD&SD	47 (10.5%)	62 (13.8%)	
PR&CR	176 (39.2%)	164 (36.5%)	
Location within the lung, n (%)			0.793
Central Lung	28 (14.7%)	35 (18.4%)	
Peripheral Lung	59 (31.1%)	68 (35.8%)	
Right	160 (30.5%)	157 (30%)	
Residual tumor, n (%)			0.280
R0	190 (50.8%)	167 (44.7%)	
R1	4 (1.1%)	9 (2.4%)	
R2	2 (0.5%)	2 (0.5%)	
DSS event, n (%)			0.219
No	197 (39.2%)	186 (37%)	
Yes	54 (10.7%)	66 (13.1%)	
PFI event, n (%)			0.236
No	163 (30.2%)	150 (27.8%)	
Yes	106 (19.7%)	120 (22.3%)	

3.2. Upregulated ADAR expression in LUAD

To elucidate the expression profile of ADAR, we extracted the transcriptomic data of cancer tissues and matched adjacent normal tissues from two publicly available repositories, TCGA and UCSC XENA. Overall, ADAR expression was aberrantly regulated in multiple cancer types, as evidenced by the significantly altered expression levels in non-paired t-tests of 33 cancers and in paired t-tests of 23 cancers. Specifically, ADAR was upregulated in several types of cancer, including bladder cancer, breast cancer, bile duct cancer, liver hepatocellular carcinoma, LUAD and stomach adenocarcinoma, yet was downregulated in kidney chromophobe (Figure 1).

To determine whether ADAR expression was perturbed in LUAD, we used t-tests to compare the ADAR mRNA expression levels of between LUAD ($n = 539$) and normal lung tissues ($n = 59$) from TCGA dataset. Our findings showed an ostensible increase in ADAR expression in LUAD tissues compared to that in normal tissues ($p < 0.001$, Figure 2A). To expand the cohort size of the normal group, we assimilated 347 normal lung specimens from the GTEx and TCGA datasets to objectively compare ADAR expression levels. Impressively, ADAR expression was still found to be significantly unregulated in the landscape of LUAD ($p < 0.001$, Figure 2B). We corroborated this conclusion by performing a paired analysis ($p < 0.001$; Figure 2C). Remarkably, the high AUC value (0.853) signified the accuracy of tumor diagnosis based on ADAR expression (Figure 2D). Based on the immunohistochemical images of ADAR expression in LUAD tissues from the HPA database, augmented expression of ADAR protein was detected in LUAD tissues (Figure 2E,F). Consequently, we can conclude that ADAR is unambiguously upregulated at both the transcriptional and translational levels in LUAD tissues.

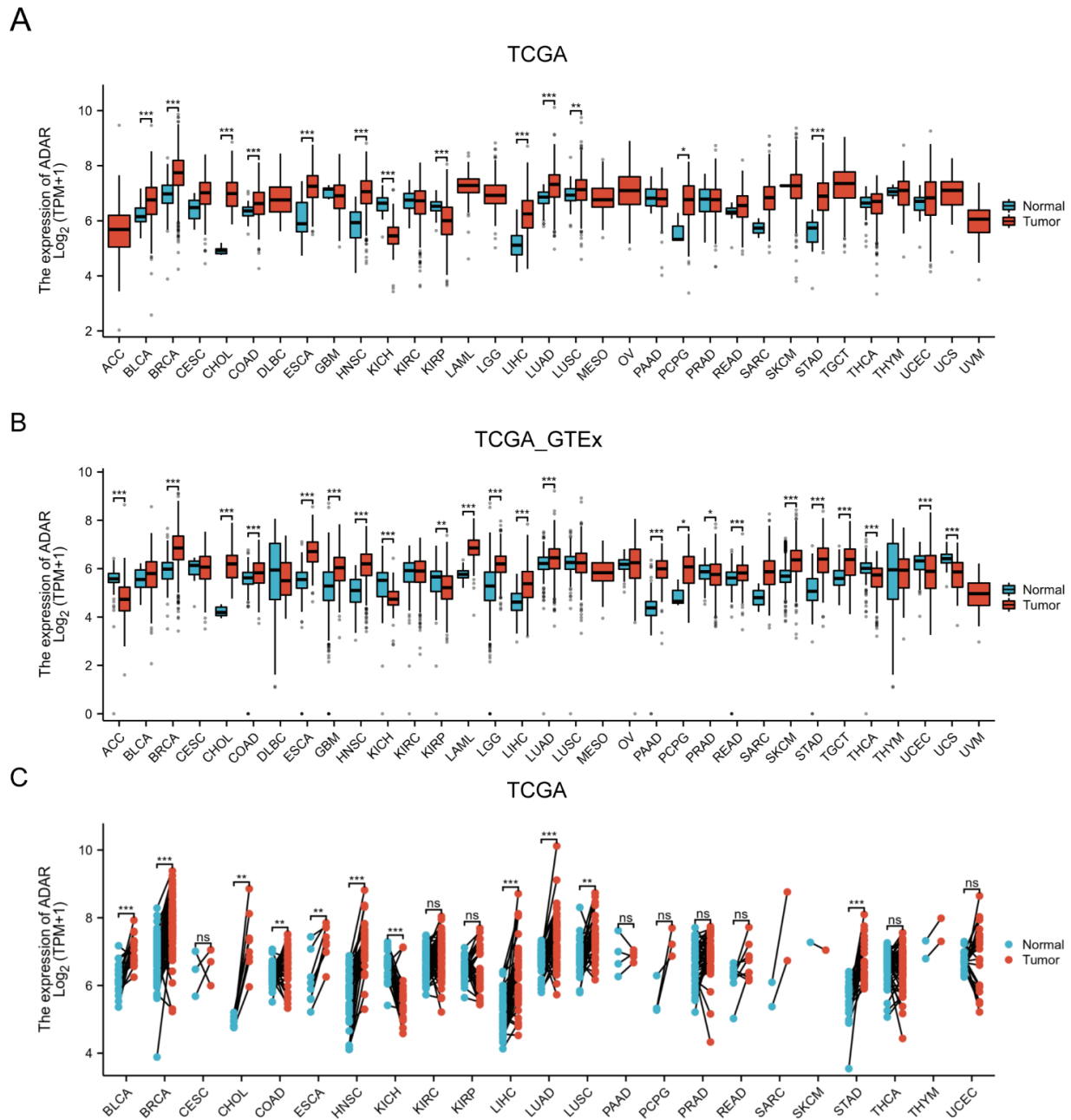


Figure 1. A pan-cancer analysis of ADAR mRNA levels reveals aberrant expression across various types of cancer. (A) ADAR expression analyzed in 33 types of cancer and normal tissues using data from TCGA database. (B) ADAR expression analyzed in 33 types of cancer and normal tissues using data from the TCGA_GTEx database. (C) Differential expression of ADAR between 23 types of tumors and their adjacent normal tissues using data from TCGA database. Tumor abbreviation names are derived from TCGA. (ns, $p > 0.05$; * $p < 0.05$; ** $p < 0.01$; *** $p < 0.001$).

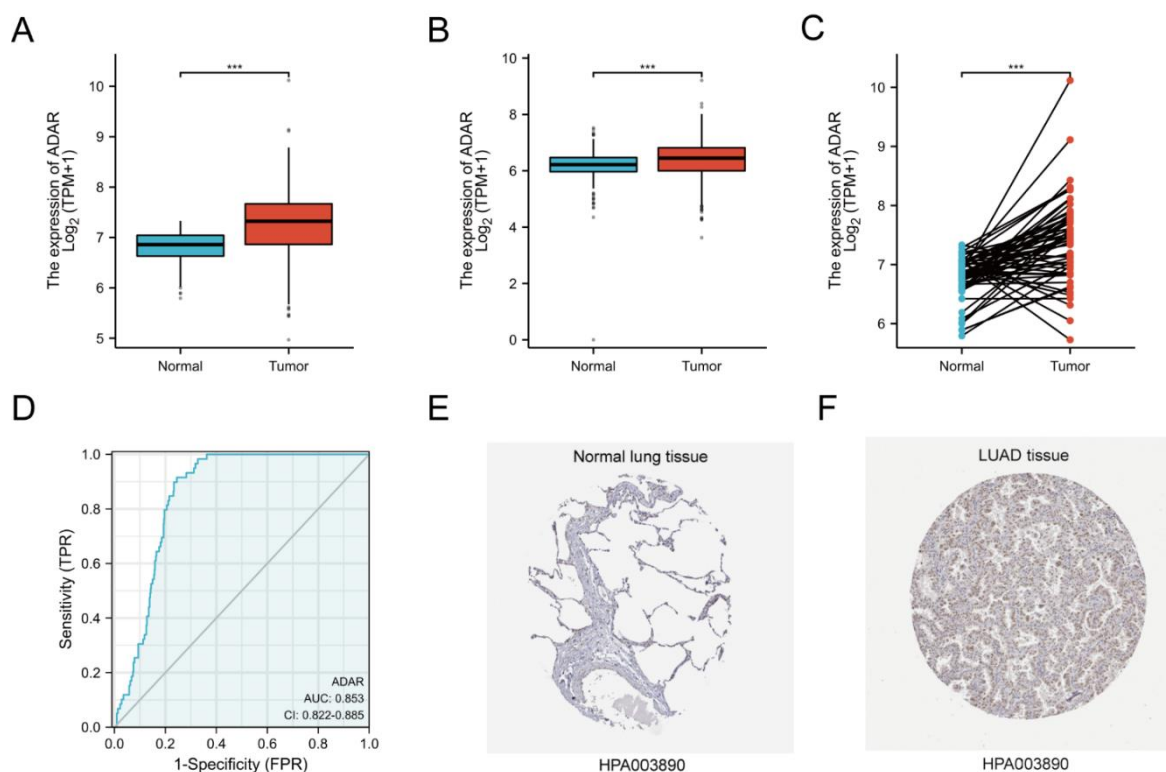


Figure 2. Comparisons at the mRNA and protein levels showed that ADAR expression was enhanced in tumor tissues. (A) Expression of ADAR in lung tumor and adjacent normal tissues from TCGA. (B) Expression of ADAR in tumor specimens of TCGA and normal lung specimens of the GTEx combined with TCGA. (C) A paired analysis of ADAR expression in LUAD and normal lung tissues from TCGA. (D) The ROC curve analysis demonstrated that ADAR expression exhibited superior accuracy in diagnosing tumors. X-axis represents false positive rate and Y-axis represents true positive rate. (E and F) Immunohistochemistry from the HPA database depicts strong ADAR protein expression in LUAD tumor tissues. (* $p < 0.05$, ** $p < 0.01$, *** $p < 0.001$).

3.3. Evaluation of ADAR expression as a predictor of poor prognosis in LUAD

The time-dependent ROC curve is a graphical tool used to evaluate the performance of classification models. If a variable exhibited a propensity to facilitate the occurrence of events, its corresponding AUC value exceeds 0.5. First, we plotted time-dependent ROC curves for ADAR expression to predict OS, DSS and PFI at 1-, 3- and 5-years. With resulting AUC values ranging from 0.5 to 0.6 for ADAR, its contribution to disease progression and mortality was indicated, but with only modest predictive performance as a single variable (Figure 3). The Kaplan-Meier method was employed to plot survival curves, allowing for a comparison of the survival times between the high- and low-ADAR expression groups. The results indicated that higher expression of ADAR was linked to shortened OS ($p = 0.019$, Figure 4).

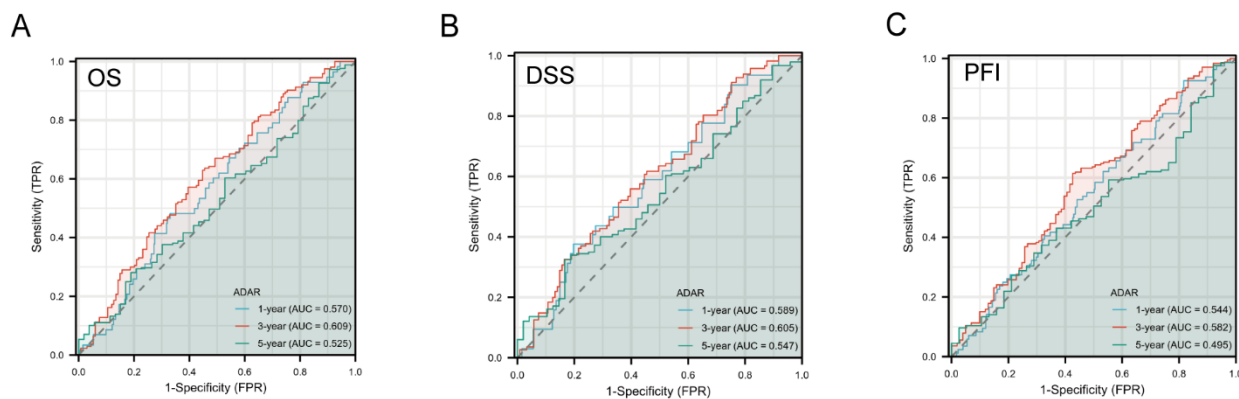


Figure 3. Time-dependent ROC curves demonstrate the ability of ADAR expression to predict OS (A), DSS (B) and PFI (C) of patients with LUAD 1, 3 and 5 years after diagnosis.

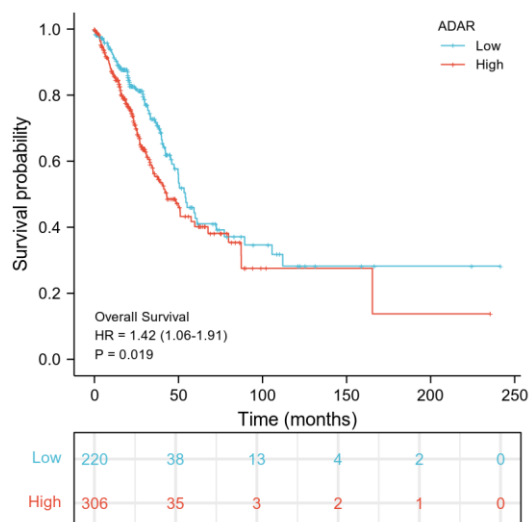


Figure 4. The survival curve was calculated using the minimum p -value method to illustrate the relationship between the OS of patients with LUAD and the ADAR expression level. The median survival time of patients in the high-ADAR expression group was significantly shorter than those with low-ADAR expression ($p = 0.019$).

Additionally, Cox univariate and multivariate analyses were conducted to evaluate OS-related variables, as presented in Table 2 and Figure 5. Univariate models showed that T-stage ($p = 0.002$), N-stage ($p < 0.001$), M-stage ($p > 0.006$), pathological stage ($p < 0.001$), primary treatment outcome ($p < 0.001$), residual tumor ($p < 0.01$) and ADAR expression ($p = 0.027$) were all significantly associated with OS. Multivariate analysis revealed that pathological stage ($p = 0.022$, HR = 2.005), residual tumor ($p = 0.007$, HR = 3.428), primary treatment outcome ($p < 0.001$, HR = 0.313) and ADAR expression ($p = 0.023$, HR = 1.698) were independent risk or protective factors that correlated with the survival time of patients with LUAD. Finally, a column plot was created based on these four variables to estimate the survival probability at 1, 3 and 5 years after diagnosis (Figure 6A). The C-index reflects

the predictive performance of the column plot, with a value closer to one indicating a more accurate prediction. A C-index value of 0.70 proved that the column plot model had a high degree of accuracy in predicting the survival rate of patients with LUAD (Figure 6B).

Table 2. Univariate and multivariate Cox regression analyses of clinical characteristics associated with overall survival.

Characteristics	Univariate analysis		Multivariate analysis	
	Hazard ratio (95% CI)	P value	Hazard ratio (95% CI)	P value
Age (> 65 vs. ≤ 65)	1.223 (0.916–1.635)	0.172		
Sex (Male vs. Female)	1.070 (0.803–1.426)	0.642		
Smoker (Yes vs. No)	0.894 (0.592–1.348)	0.591		
Race (Asian & Black or African American vs. White)	0.678 (0.415–1.109)	0.121		
T stage (T2&T3&T4 vs. T1)	1.728 (1.229–2.431)	0.002	1.252 (0.730–2.147)	0.414
N stage (N1&N2&N3 vs. N0)	2.601 (1.944–3.480)	< 0.001	1.422 (0.879–2.302)	0.151
M stage (M1 vs. M0)	2.136 (1.248–3.653)	0.006	0.941 (0.356–2.488)	0.902
Pathologic stage (III&IV vs. I&II)	2.664 (1.960–3.621)	< 0.001	2.005 (1.104–3.641)	0.022
Location within lung (Peripheral vs. Central)	0.913 (0.570–1.463)	0.706		
Residual tumor (R1&R2 vs. R0)	3.879 (2.169–6.936)	< 0.001	3.428 (1.397–8.410)	0.007
Primary therapy outcome (PR&CR vs. PD&SD)	0.377 (0.268–0.530)	< 0.001	0.313 (0.188–0.521)	< 0.001
ADAR (High vs. Low)	1.384 (1.038–1.846)	0.027	1.698 (1.075–2.680)	0.023

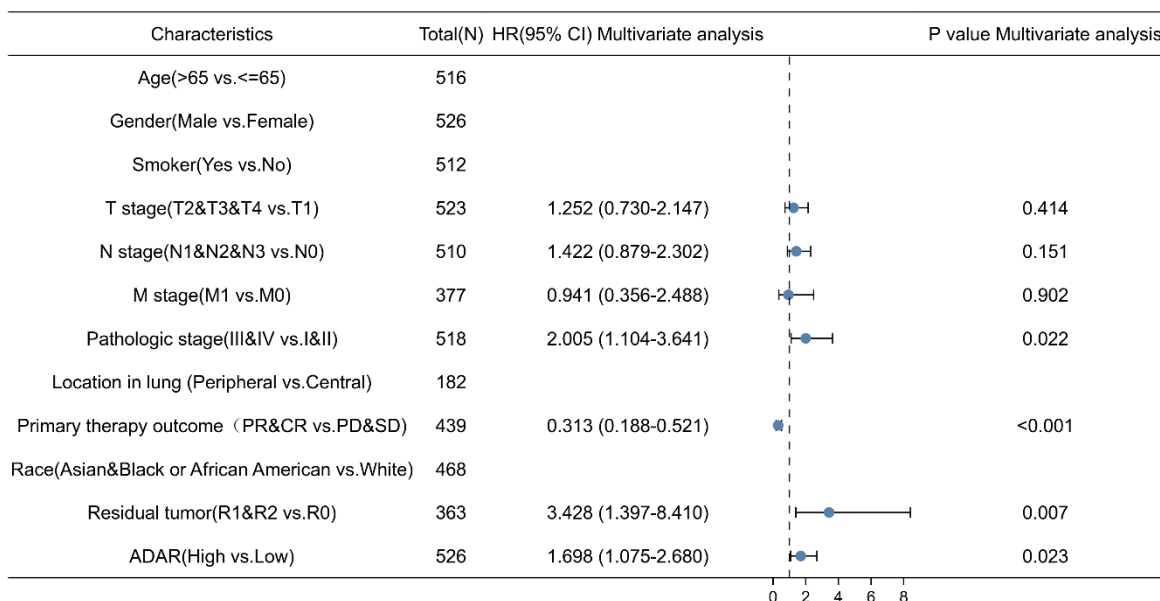
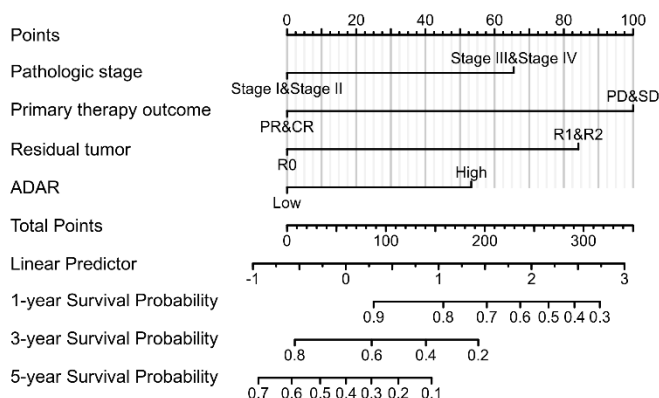


Figure 5. Forest plot of the multivariate Cox regression analysis of patients with LUAD.

A



B

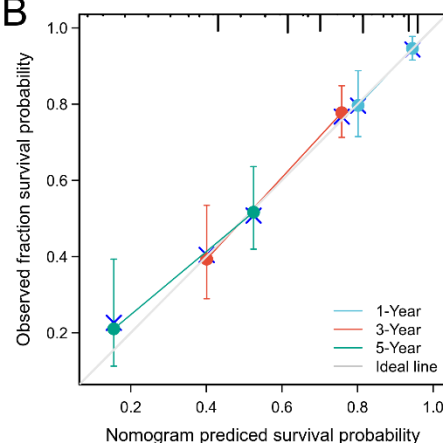


Figure 6. Effects of ADAR and other clinical factors on OS of patients with LUAD. (A) A nomogram for predicting the probability of 1-, 3- and 5-year survival time for patients with LUAD. (B) Calibration plots are used to observe the accuracy of the nomogram model in predicting survival probability.

3.4. DEGs between patients with high- and low-ADAR expression

The 539 patients diagnosed with LUAD were divided into high- and low-expression cohorts based on their ADAR expression levels. Our subsequent exploration using single-gene differential analysis revealed 1,395 DEGs that satisfied our criteria of $|\log FC| > 1.5$ and $p < 0.05$, comprising 83 downregulated genes and 1,312 upregulated genes (Figure 7A). Interestingly, among these genes, we detected a preponderance of lncRNAs, totaling 482, followed by processed pseudogenes, totaling 402. We further visualized the 10 most upregulated and 10 most downregulated DEGs using a heatmap (Figure 7B).

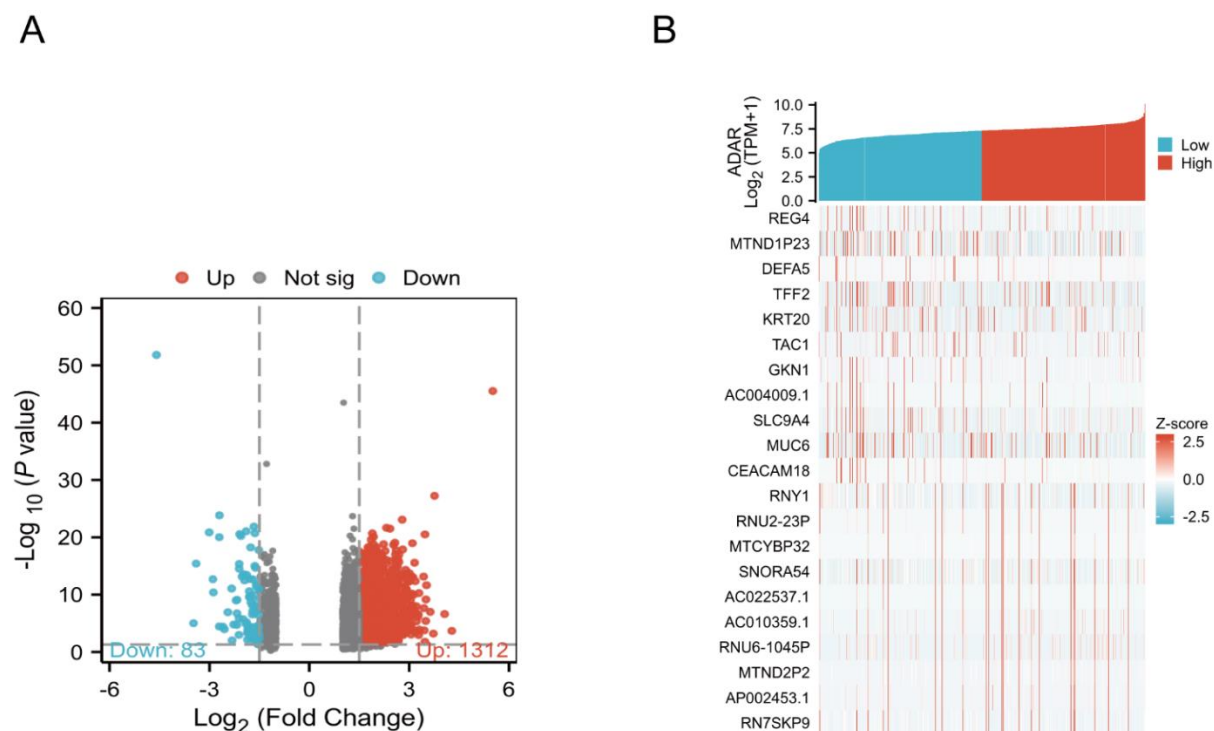


Figure 7. DEGs identified between the high- and low-ADAR expression patients with LUAD. (A) DEGs illustrated by a volcano plot to highlight both up- and down-regulated genes. (B) A heatmap constructed to show the 20 most notable DEGs.

3.5. Relationship between ADAR expression and immune cell infiltration in LUAD

The current study revealed that ADAR actively participates in regulating immune responses during tumorigenesis and has a profound and consequential impact on the prognosis of patients with cancer. Thus, with further investigation into the relationship between ADAR expression and immune cell infiltration in LUAD, our findings revealed that ADAR upregulation is closely associated with increased infiltration of T central memory (Tcm), T helper 2 (Th2), T helper, T effector memory (Tem) and activated dendritic (aDc) cells into the tumor microenvironment. Conversely, ADAR expression was also associated with reduced infiltration of the mast, NK CD56bright, CD8 T, plasmacytoid dendritic (pDC), immature dendritic (iDC) and B cells (Figure 8A). Furthermore, the largest increase in infiltration was found in Tcm cells ($R = 0.253$, $p < 0.001$, Figure 8B), followed by Th2 cells ($R = 0.214$, $p < 0.001$, Figure 8C) and T helper cells ($R = 0.187$, $p < 0.001$, Figure 8D). In contrast, a highly significant decrease in the infiltration of pDc ($R = -0.135$, $p = 0.002$, Figure 7E), iDc ($R = -0.159$, $p < 0.001$, Figure 8F) and B cells ($R = -0.210$, $p < 0.001$, Figure 8G) into the tumor microenvironment was observed.

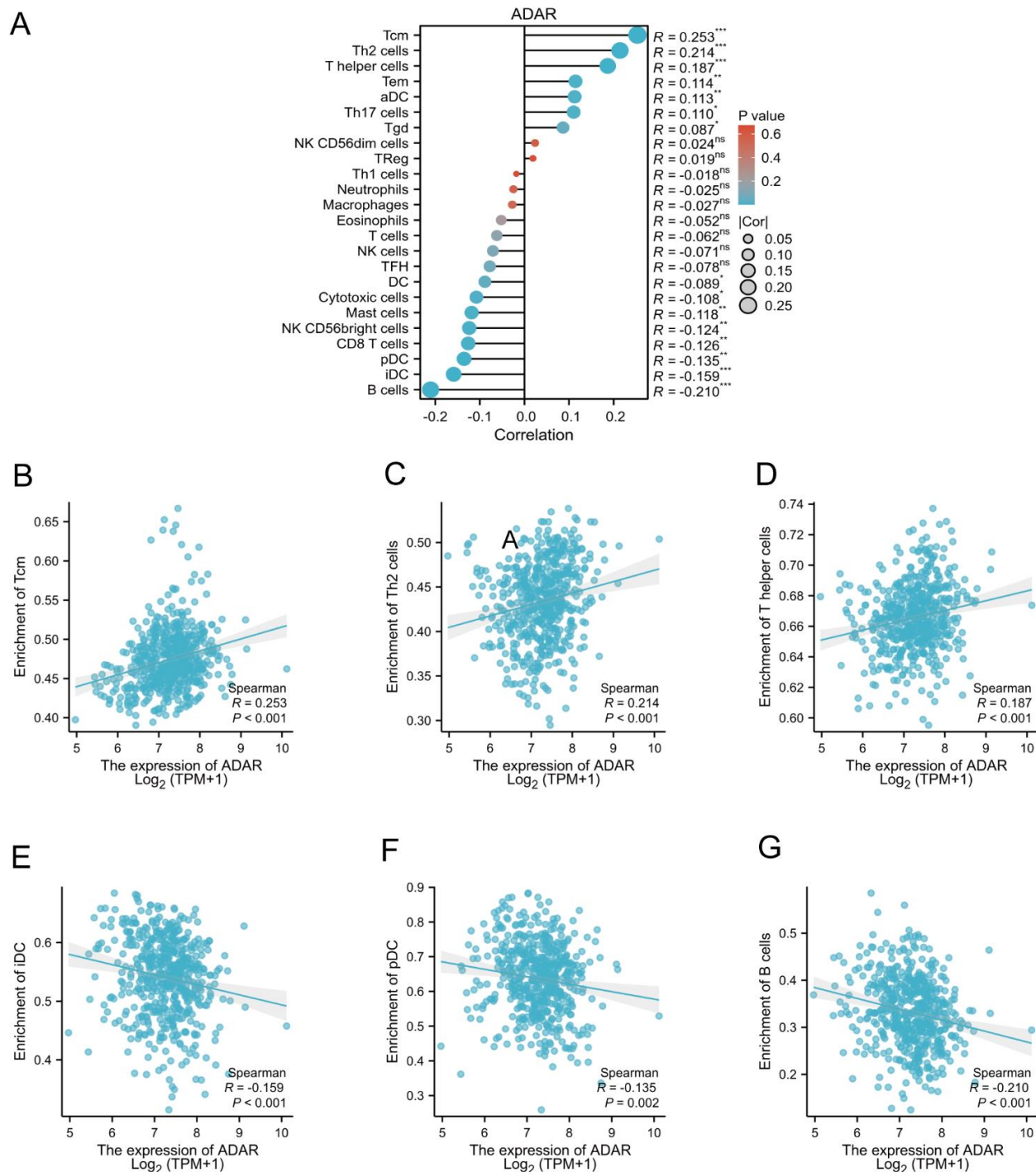


Figure 8. Relationship between ADAR expression and immune cell infiltration into the tumor microenvironment of LUAD. (A) The lollipop diagrams show the correlation between ADAR expression level and the abundance of 24 different immune cells. The size of dots indicates the absolute value of Spearman r . Positive correlations were detected between ADAR expression levels and Tcm cells, Th2 cells and T helper cells (B, C, D). Negative correlations were observed between ADAR expression levels and iDC, pDC and B cells (E, F, G).

3.6. PPI network and functional enrichment analyses of the top 100 genes associated with ADAR

To delve deeper into the intricate mechanisms of ADAR in neoplastic tissues, we retrieved a comprehensive list of the 100 genes most highly associated with ADAR from the GEPIA2 database, revealing potential avenues for its interplay in tumorigenesis. PPI analysis is a crucial tool for studying gene regulatory networks, helping us understand how genes interact and associate with each other at the protein level. The list of genes was subjected to PPI analysis using the STRING website, followed by visualization using Cytoscape software. This analysis yielded a PPI network consisting of 74 nodes and 131 interdependent relationships, which were subsequently searched for densely connected regions to identify hub genes (Figure 9A). Hub gene selection was facilitated using the Mcode plugin, resulting in the identification of three distinct clusters. The cluster score reflects the tightness of the connections within the cluster, with a higher score indicating stronger interactions among the genes in the cluster. Clustering analysis revealed that Cluster 1, with a score of 7.2, contained 11 genes (*UPF2*, *SRSF1*, *RBM8A*, *FUBP1*, *TARDBP*, *HNRNPU*, *BCLAF1*, *CPSF6*, *HNRNPK*, *CHTOP* and *RB15*) and 33 edges, whereas Cluster 2, which scored 4.0, contained 4 genes (*TRIP12*, *POGZ*, *UBQLN1* and *UBQLN4*) and 11 edges (Figure 9C,D). Finally, Cluster 3, which scored 3.0, comprised only 3 genes (*ARHGEF11*, *IQGAP3* and *GPATCH4*) and 3 edges (Figure 9E).

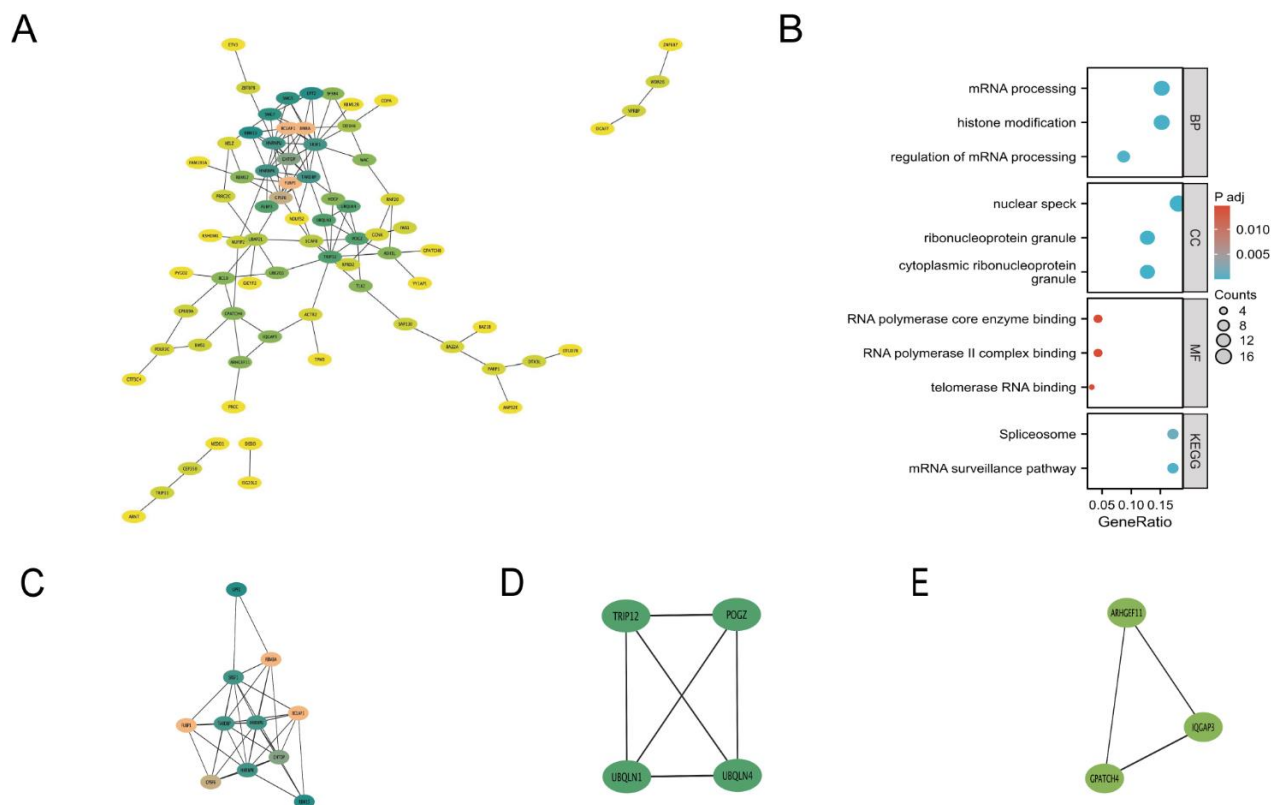


Figure 9. The interplay between the top 100 genes that exhibit the highest degree of correlation with ADAR, as ascertained from the GEPIA2 database. (A) PPI regulatory diagram of these 100 genes. (B) GO/KEGG enrichment analysis for the same set of genes. (C–E) The top 3 modules constructed from the PPI network of these 100 genes.

To highlight the potential functional ramifications of dysregulated genes linked to ADAR in tumors, we performed GO and KEGG pathway analyses. Our GO analysis revealed that ADAR may participate in numerous biological processes, including histone modification, mRNA processing and regulation of mRNA processing, with potential molecular locations in the nuclear speck, ribonucleoprotein granules and cytoplasmic ribonucleoprotein granules, and potential molecular functions, such as RNA polymerase II complex binding, telomerase RNA binding and RNA polymerase core enzyme binding. Additionally, our KEGG pathway enrichment analysis revealed the crucial involvement of ADAR in pivotal molecular pathways such as the mRNA surveillance pathway and spliceosomes (Figure 9B). These findings suggest that ADAR is likely involved in the regulation of transcription through histone modification in the nucleus, whereas it potentially participates in the synthesis, processing and regulation of mRNA within ribonucleoprotein granules in the cytoplasm.

4. Discussion

Lung cancer is the deadliest cancer worldwide [27]. With the advent of molecular-targeted therapy and immunotherapy, a small subset of patients has shown prolonged survival. However, outcomes in most patients with advanced lung cancer remain unsatisfactory. Therefore, it is crucial to identify effective biomarkers to help guide diagnosis, support treatment decisions and predict prognosis.

ADARs are a family of enzymes that play a critical role in the predominant form of RNA editing in mammals, wherein they catalyze the conversion of adenosines to inosines in dsRNA [28]. There are two major ADAR1 isoforms: the IFN-inducible isoform p150 and the shorter constitutive isoform p110 [29]. Upon detection of unedited endogenous dsRNA molecules by host sensors, such as MDA5 and PKR, cells activate the IFN response. Concurrently, ADAR1 p150 is also activated to inhibit the hyperactivation of MAD5 or PKR during this response [30]. A pivotal function of ADAR1 is to maintain the balance between immune activation and self-tolerance. A-to-I editing affects several biological processes. Using bioinformatic analyses and high-throughput sequencing approaches, researchers have identified an extensive repertoire of editing sites distributed across various genomic regions, including both the coding and non-coding regions of mRNA. As a post-transcriptional modification, mRNA editing diversifies transcripts and proteomes [31]. In studies examining the RNA editing sites in coding regions, these activities affect tumor progression, as observed in *AZINI*, *METTL* and *COPA* [17,32–34]. However, it should be noted that the majority of A-to-I RNA editing sites are located in non-coding sequences [35], such as in microRNAs, lncRNAs and circular RNAs, which also participate in the direct or indirect regulation of tumor growth and invasion [36–38]. In thyroid cancer, ADAR1 mediates the over-editing of mir-200, leading to the upregulation of the target gene *ZEB1*, promoting the epithelial-mesenchymal transition. Furthermore, the tumor-forming ability of ADAR1 knockout cells is diminished [39]. Altering the expression level of ADAR influences the expression of the lncRNA LINC00944, which is associated with adverse prognoses in patients with breast cancer [40]. ADAR1 suppressed the expression of hsa_circ_0004872, consequently promoting the invasiveness and metastatic potential of gastric cancer cells [41]. Thus, A-to-I RNA editing, a potentially useful marker for cancer prognosis and therapy, would likely be of great benefit in the field of oncology. In our investigation, we compared ADAR expression levels between various tumor types and their corresponding normal tissues using publicly available gene data obtained from TCGA database. Our study demonstrated that ADAR displays altered expression patterns in a variety of tumor types, including LUAD. Furthermore, high ADAR expression has been linked to poor patient prognosis,

advanced pathological stage, residual tumors and suboptimal primary therapy outcomes. Nevertheless, the predictive performance of ADAR as a standalone risk factor was modest. These results suggest that, when combined with certain clinical characteristics, ADAR can serve as a valuable prognostic marker for predicting the outcome of LUAD.

Moreover, loss of ADAR1 activates the IFN pathway mediated by MDA5 and PKR, thereby sensitizing tumors to ICBs and overcoming resistance to anti-PD-1 therapy [21]. Studies have demonstrated that ADAR can serve as a mediator of ZBP1-induced necrosis by inhibiting the accumulation of endogenous Z-RNA, consequently obstructing tumor immunogenicity and leading to immune therapy failure [42]. Therefore, ADAR is a promising target for overcoming immunotherapy resistance. Currently, the response rate of lung cancer to ICBs is approximately 20%, indicating the efficacy of immunotherapy must be improved [43,44]. A major finding of our study was that ADAR levels correlated with indicators of immune infiltration in LUAD. The infiltrations of Tcm, Th2 and T helper cells were positively correlated, while those of iDc, pDc and B cells were negatively correlated with ADAR levels in LUAD. This implies that ADAR is primarily involved in modulating the infiltration of T cell subsets, influencing antigen presentation and activating B cells to exert immunosuppressive effects.

Furthermore, we also examined the biological mechanisms of ADAR and discovered that among the 1395 significantly altered genes that were potentially regulated by ADAR, nearly one-third were lncRNAs and the majority were non-coding RNAs, indicating that ADAR primarily operates in non-coding domains. This finding is in agreement with past results reported in the literature. Subsequent functional and pathway enrichment analyses demonstrated that ADAR is predominantly involved in epigenetic regulation such as mRNA processing and histone modification. This indicates that ADAR primarily exerts its regulatory effects at both transcriptional and post-transcriptional levels. Thus, our study provides insights into the potential involvement of ADAR in tumor immune infiltration and highlights its potential utility as a biomarker for cancer diagnosis, treatment and prognosis.

Although this study contributed to our understanding of the relationship between ADAR and LUAD, some areas warrant further improvement. First, although we observed an association between increased ADAR and shorter patient survival, a specific predictive model for patient prognosis based on clinical characteristics and ADAR expression was not implemented in this study and requires further investigation. Second, we explored the potential mechanisms through which ADAR may promote lung cancer progression by impacting gene transcription through histone modifications and mRNA processing via the nucleolus, ultimately influencing tumor immunity by modulating T-cell subsets. However, these conclusions are based on indirect evidence and inferences. Additional *in vitro* and *in vivo* experiments, as well as clinical research, are necessary to confirm whether ADAR contributes to tumor development in LUAD by regulating immune tolerance. For example, in the future, we can validate the role of ADAR deficiency in overcoming immune tolerance in cancer-bearing mice at the animal level and investigate the specific mechanisms at the cellular level, such as through the regulation of non-coding RNA and histone modifications. Moreover, through spaCI technology, we will be able to elucidate the intricate intercellular communication pathways employed by tumor cells exhibiting heightened ADAR expression and their interaction with immune cells [45]. Additionally, due to the lack of treatment description in TCGA database, it would be necessary to conduct a prospective clinical study to evaluate the impact of ADAR on the clinical prognosis of patients undergoing anti-PD-1 therapy, if deemed necessary.

5. Conclusions

This study represents a novel contribution to the literature as it is the first to propose a potential role for ADAR in the pathogenesis and progression of LUAD, allowing it to serve as a novel prognostic indicator. Our analysis revealed a significant correlation between elevated ADAR expression and poor prognosis in patients with LUAD. This is supported by the infiltration of Tcm and other immune cells into the tumor microenvironment. However, experimental confirmation is required to clarify these biological mechanisms and effects of ADAR in patients with LUAD.

Use of AI tools declaration

The authors declare they have not used Artificial Intelligence (AI) tools in the creation of this article.

Authors contributions

SH: research idea, data acquisition, data analysis, results visualization and manuscript writing. FW, JY: assist in data analysis and manuscript writing. XX: research idea, research purpose, research method and result presentation. All authors participated in the study and approved the final manuscript.

Acknowledgements

We would like to acknowledge the financial support provided by The Research Fund of Northern Jiangsu People's Hospital (grant number SBLC22002).

Conflict of Interest

The authors declare there is no conflict of interest.

References

1. C. Jin, G. K. Lagoudas, C. Zhao, S. Bullman, A. Bhutkar, B. Hu, et al., Commensal microbiota promote lung cancer development via $\gamma\delta$ T cells, *Cell*, **176** (2019), 998–1013. <https://doi.org/10.1016/j.cell.2018.12.040>
2. J. Huo, Y. Xu, T. Sheu, R. J. Volk, Y. T. Shih, Complication rates and downstream medical costs associated with invasive diagnostic procedures for lung abnormalities in the community setting, *JAMA Int. Med.*, **179** (2019), 324–332. <https://doi.org/10.1001/jamainternmed.2018.6277>
3. R. K. Meleppat, C. R. Fortenbach, Y. Jian, E. S. Martinez, K. Wagner, B. S. Modjtahedi, et al., In vivo imaging of retinal and choroidal morphology and vascular plexuses of vertebrates using swept-source optical coherence tomography, *Transl. Vis. Sci. Technol.*, **11** (2022), 11. <https://doi.org/10.1167/tvst.11.8.11>
4. R. K. Meleppat, K. E. Ronning, S. J. Karlen, M. E. Burns, E. N. Pugh, R. J. Zawadzki, In vivo multimodal retinal imaging of disease-related pigmentary changes in retinal pigment epithelium, *Sci. Rep.*, **11** (2021), 16252. <https://doi.org/10.1038/s41598-021-95320-z>

5. K. S. Blandin, P. A. Crosbie, H. Balata, J. Chudziak, T. Hussell, C. Dive, Progress and prospects of early detection in lung cancer, *Open Biol.*, **7** (2017), 170070. <https://doi.org/10.1098/rsob.170070>
6. P. C. Hoffman, A. M. Mauer, E. E. Vokes, Lung cancer, *Lancet*, **355** (2000), 479–485. [https://doi.org/10.1016/S0140-6736\(00\)82038-3](https://doi.org/10.1016/S0140-6736(00)82038-3)
7. S. M. Park, E. Y. Choi, M. Bae, S. Kim, J. B. Park, H. Yoo, et al., Histone variant H3F3A promotes lung cancer cell migration through intronic regulation, *Nat. Commun.*, **7** (2016), 12914. <https://doi.org/10.1038/ncomms12914>
8. B. L. Bass, RNA editing by adenosine deaminases that act on RNA, *Annu. Rev. Biochem.*, **71** (2002), 817–846. <https://doi.org/10.1146/annurev.biochem.71.110601.135501>
9. L. Bazak, A. Haviv, M. Barak, J. H. Jacob, P. Deng, R. Zhang, et al., A-to-I RNA editing occurs at over a hundred million genomic sites, located in a majority of human genes, *Genome Res.*, **24** (2014), 365–376. <https://doi.org/10.1101/gr.164749.113>
10. K. Licht, U. Kapoor, F. Amman, E. Picardi, D. Martin, P. Bajad, et al., A high resolution A-to-I editing map in the mouse identifies editing events controlled by pre-mRNA splicing, *Genome Res.*, **29** (2019), 1453–1463. <https://doi.org/10.1101/gr.242636.118>
11. K. Pestal, C. C. Funk, J. M. Snyder, N. D. Price, P. M. Treuting, D. B. Stetson, Isoforms of RNA-editing enzyme adar1 independently control nucleic acid sensor MDA5-driven autoimmunity and multi-organ development, *Immunity*, **43** (2015), 933–944. <https://doi.org/10.1016/j.immuni.2015.11.001>
12. B. J. Liddicoat, A. M. Chalk, C. R. Walkley, ADAR1, inosine and the immune sensing system: distinguishing self from non-self, *Wiley. Interdiscip. Rev. RNA.*, **7** (2016), 157–172. <https://doi.org/10.1002/wrna.1322>
13. B. J. Liddicoat, R. Piskol, A. M. Chalk, G. Ramaswami, M. Higuchi, J. C. Hartner, et al., RNA editing by ADAR1 prevents MDA5 sensing of endogenous dsRNA as nonself, *Science*, **349** (2015), 1115–1120. <https://doi.org/10.1126/science.aac7049>
14. G. I. Rice, P. R. Kasher, G. M. Forte, N. M. Mannion, S. M. Greenwood, M. Szykiewicz, et al., Mutations in ADAR1 cause Aicardi-Goutières syndrome associated with a type I interferon signature, *Nat. Genet.*, **44** (2012), 1243–1248. <https://doi.org/10.1038/ng.2414>
15. Y. Miyamura, T. Suzuki, M. Kono, K. Inagaki, S. Ito, N. Suzuki, et al., Mutations of the RNA-specific adenosine deaminase gene (DSRAD) are involved in dyschromatosis symmetrica hereditaria, *Am. J. Hum. Genet.*, **73** (2003), 693–699. <https://doi.org/10.1086/378209>
16. X. J. Zhang, P. P. He, M. Li, C. D. He, K. L. Yan, Y. Cui, et al., Seven novel mutations of the ADAR gene in Chinese families and sporadic patients with dyschromatosis symmetrica hereditaria (DSH), *Hum. Mutat.*, **23** (2004), 629–630. <https://doi.org/10.1002/humu.9246>
17. T. H. Chan, C. H. Lin, L. Qi, J. Fei, Y. Li, K. J. Yong, et al., A disrupted RNA editing balance mediated by ADARs (Adenosine De Aminases that act on RNA) in human hepatocellular carcinoma, *Gut*, **63** (2014), 832–843. <https://doi.org/10.1136/gutjnl-2012-304037>
18. L. Han, L. Diao, S. Yu, X. Xu, J. Li, R. Zhang, et al., The genomic landscape and clinical relevance of A-to-I RNA editing in human cancers, *Cancer Cell*, **28** (2015), 515–528. <https://doi.org/10.1016/j.ccell.2015.08.013>
19. X. Peng, X. Xu, Y. Wang, D. H. Hawke, S. Yu, L. Han, et al., A-to-I RNA editing contributes to proteomic diversity in cancer, *Cancer Cell*, **35** (2018), 817–828. <https://doi.org/10.1016/j.ccell.2018.03.026>

20. H. Liu, J. Golji, L. K. Brodeur, F. S. Chung, J. T. Chen, R. S. deBeaumont, et al., Tumor-derived IFN triggers chronic pathway agonism and sensitivity to ADAR loss, *Nat. Med.*, **25** (2019), 95–102. <https://doi.org/10.1038/s41591-018-0302-5>
21. J. J. Ishizuka, R. T. Manguso, C. K. Cheruiyot, K. Bi, A. Panda, A. V. Iracheta, et al., Loss of ADAR1 in tumours overcomes resistance to immune checkpoint blockade, *Nature*, **565** (2019), 43–48. <https://doi.org/10.1038/s41586-018-0768-9>
22. K. Fritzell, L. D. Xu, M. Otrocka, C. Andréasson, M. Öhman, Sensitive ADAR editing reporter in cancer cells enables high-throughput screening of small molecule libraries, *Nucleic Acids Res.*, **47** (2019), 22. <https://doi.org/10.1093/nar/gky1228>
23. J. Vivian, A. A. Rao, F. A. Nothhaft, C. Ketchum, J. Armstrong, A. Novak, et al., Toil enables reproducible, open source, big biomedical data analyses, *Nat. Biotechnol.*, **35** (2017), 314–316. <https://doi.org/10.1038/nbt.3772>
24. M. Uhlén, L. Fagerberg, B. M. Hallström, C. Lindskog, P. Oksvold, A. Mardinoglu, et al., Tissue-based map of the human proteome, *Science*, **347** (2015), 1260419. <https://doi.org/10.1126/science.1260419>
25. S. Hänzelmann, R. Castelo, J. Guinney, GSEA: Gene set variation analysis for microarray and RNA-seq data, *BMC. Bioinf.*, **14** (2013), 7. <https://doi.org/10.1186/1471-2105-14-7>
26. Z. Tang, B. Kang, C. Li, T. Chen, Z. Zhang, GEPIA2: An enhanced web server for large-scale expression profiling and interactive analysis, *Nucleic Acids Res.*, **47** (2019), w556–w560. <https://doi.org/10.1093/nar/gkz430>
27. R. S. Herbst, J. V. Heymach, S. M. Lippman, Lung cancer, *N. Engl. J. Med.*, **359** (2008), 1367–1380. <https://doi.org/10.1056/NEJMra0802714>
28. B. J. Booth, S. Nourreddine, D. Katrekar, Y. Savva, D. Bose, T. J. Long, et al., RNA editing: Expanding the potential of RNA therapeutics, *Mol. Ther.*, **31** (2023), 533–549. <https://doi.org/10.1016/j.ymthe.2023.01.005>
29. B. Song, Y. Shiromoto, M. Minakuchi, K. Nishikura, The role of RNA editing enzyme ADAR1 in human disease, *Wiley. Interdiscip. Rev. RNA*, **13** (2022), 1665. <https://doi.org/10.1002/wrna.1665>
30. J. Quin, J. Sedmik, D. Vukić, A. Khan, L. P. Keegan, M. A. O'Connell, ADAR RNA modifications, the epitranscriptome and innate immunity, *Trends. Biochem. Sci.*, **46** (2021), 758–771. <https://doi.org/10.1016/j.tibs.2021.02.002>
31. G. Lev-Maor, R. Sorek, E. Y. Levanon, N. Paz, E. Eisenberg, G. Ast, RNA-editing-mediated exon evolution, *Genome Biol.*, **8** (2007), 29. <https://doi.org/10.1186/gb-2007-8-2-r29>
32. L. Chen, Y. Li, C. H. Lin, T. H. Chan, R. K. Chow, Y. Song, et al., Recoding RNA editing of AZIN1 predisposes to hepatocellular carcinoma, *Nat. Med.*, **19** (2013), 209–216. <https://doi.org/10.1038/nm.3043>
33. S. Takeda, K. Shigeyasu, Y. Okugawa, K. Yoshida, Y. Mori, S. Yano, et al., Activation of AZIN1 RNA editing is a novel mechanism that promotes invasive potential of cancer-associated fibroblasts in colorectal cancer, *Cancer Lett.*, **444** (2019), 127–135. <https://doi.org/10.1016/j.canlet.2018.12.009>
34. Y. Li, N. X. Wang, C. Yin, S. S. Jiang, J. C. Li, S. Y. Yang, RNA editing enzyme ADAR1 regulates METTL3 in an editing dependent manner to promote breast cancer progression via METTL3/ARHGAP5/YTHDF1 Axis, *Int. J. Mol. Sci.*, **23** (2022), 9656. <https://doi.org/10.3390/ijms23179656>

35. B. A. Chua, D. W. Van, C. Jamieson, R. A. J. Signer, Post-Transcriptional regulation of homeostatic, stressed, and malignant stem cells, *Cell. Stem. Cell.*, **26** (2020), 138–159. <https://doi.org/10.1016/j.stem.2020.01.005>
36. D. A. Silvestris, C. Scopa, S. Hanchi, F. Locatelli, A. Gallo, De Novo A-to-I RNA editing discovery in lncRNA, *Cancers (Basel)*, **12** (2020), 2959. <https://doi.org/10.3390/cancers12102959>
37. L. Nair, H. Chung, U. Basu, Regulation of long non-coding RNAs and genome dynamics by the RNA surveillance machinery, *Nat. Rev. Mol. Cell. Biol.*, **21** (2020), 123–136. <https://doi.org/10.1038/s41580-019-0209-0>
38. H. Wang, S. Chen, J. Wei, G. Song, Y. Zhao, A-to-I RNA editing in cancer: From evaluating the editing level to exploring the editing effects, *Front Oncol.*, **10** (2020), 632187. <https://doi.org/10.3389/fonc.2020.632187>
39. J. M. Ramírez, A. R. Baker, F. J. Slack, P. Santisteban, ADAR1-mediated RNA editing is a novel oncogenic process in thyroid cancer and regulates miR-200 activity, *Oncogene*, **39** (2020), 3738–3753. <https://doi.org/10.1038/s41388-020-1248-x>
40. P. R. de Santiago, A. Blanco, F. Morales, K. Marcelain, O. Harismendy, M. H. Sjöberg, et al., Immune-related lncRNA LINC00944 responds to variations in ADAR1 levels and it is associated with breast cancer prognosis, *Life Sci.*, **268** (2021), 118956. <https://doi.org/10.1016/j.lfs.2020.118956>
41. C. Ma, X. Wang, F. Yang, Y. Zang, J. Liu, X. Wang, et al., Circular RNA HSA_CIRC_0004872 inhibits gastric cancer progression via the miR-224/Smad4/ADAR1 successive regulatory circuit, *Mol. Cancer*, **19** (2020), 157. <https://doi.org/10.1186/s12943-020-01268-5>
42. T. Zhang, C. Yin, A. Fedorov, L. Qiao, H. Bao, N. Beknazarov, et al., ADAR1 masks the cancer immunotherapeutic promise of ZBP1-driven necroptosis, *Nature*, **606** (2022), 594–602. <https://doi.org/10.1038/s41586-022-04753-7>
43. M. C. Garassino, S. Gadgeel, E. Esteban, E. Felip, G. Speranza, M. Domine, et al., Patient-reported outcomes following pembrolizumab or placebo plus pemetrexed and platinum in patients with previously untreated, metastatic, non-squamous non-small-cell lung cancer (KEYNOTE-189): A multicentre, double-blind, randomised, placebo-controlled, phase 3 trial, *Lancet Oncol.*, **21** (2020), 387–397. [https://doi.org/10.1016/s1470-2045\(19\)30801-0](https://doi.org/10.1016/s1470-2045(19)30801-0)
44. D. Fujimoto, S. Miura, K. Yoshimura, K. Wakuda, Y. Oya, T. Yokoyama, et al., Pembrolizumab plus chemotherapy-induced pneumonitis in chemo-naïve patients with non-squamous non-small cell lung cancer: A multicentre, retrospective cohort study, *Eur. J. Cancer*, **150** (2021), 63–72. <https://doi.org/10.1016/j.ejca.2021.03.016>
45. Z. Tang, T. Zhang, B. Yang, J. Su, Q. Song, spaCI: deciphering spatial cellular communications through adaptive graph model, *Brief Bioinform.*, **24** (2023), bbac563. <https://doi.org/10.1093/bib/bbac563>



AIMS Press

©2023 the Author(s), licensee AIMS Press. This is an open access article distributed under the terms of the Creative Commons Attribution License (<http://creativecommons.org/licenses/by/4.0>)